Acta Mechanica Slovaca **28 (4): 14 - 24,** December **2024**
https://doi.org/10.21496/ams.2024.018

Acta Mechanica Slovaca
ISSN 1335-2393
www.actamechanica.sk

Numerical Study of Tensile-shear Fracture Behaviour of Resistance Spot Welded Sheet Steel with DP 450 and DP 980

Cherfi Mohamed [1,*], Ait kaci Djafar [1], Moulgada Abdelmajid [1], Sahli abderahmane [1], Ghermaoui Ilias Mohammed Amine [1]

1 Department of Mechanical Engineering, Laboratory Mechanics Physics of Materials (LMPM), University of SidiBel Abbes, BP 89, cite Ben M'hidi, SidiBel Abbes, 22000, Algeria

Abstract: The use of resistance electric welding to assemble metal plates is of crucial importance in various industrial sectors. Studying the fracture behavior of resistance-welded components, especially alloys DP450 and DP980, is crucial to ensure the reliability and durability of welded structures in demanding industrial applications. When components are subjected to mechanical loads, the resulting stresses can exceed tolerable limits, leading to the initiation of damage and, ultimately, fracture. A comprehensive investigation into the fracture behavior of resistance-welded components using DP 450 and DP 980 alloys will provide a better understanding of the fracture mechanisms associated with these alloys. This will offer valuable insights for optimizing welding parameters, selecting materials, and designing components to minimize the risks of premature fracture. In this study, we will focus on the implications of the crack detected at the base metal level, as it is identified as the initial damaged material in the BM-HAZ-MM sequence. This crack, with a predefined size (10mm), will be subjected to continuous loading to analyze the evolution of the J parameter. The objective of this study is to track the crack's progression and assess its impact on material performance. By monitoring the J parameter during continuous loading, we will quantify crack advancement and gain crucial information about its propagation. This will enable us to implement preventive measures and design suitable solutions to enhance the base metal's strength. This chapter marks a significant milestone in our study, as it will provide deeper insights into the failures of the base material.

Keywords: keyword; Dual-phase, Finite Element Method, spot welding, tensile shear Strength

1. Introduction

The use of resistance electric welding to join metal plates is of crucial importance in various industrial sectors [1-2-3]. This welding method, also known as spot welding, is renowned for its speed, reliability, and ability to create strong joints between sheets [4-5]. This technique involves passing an electric current through the plates to be joined, generating heat through electrical resistance, which melts the metals at the interface. Once cooled, the metals solidify to form a sturdy junction [6]. The scope of application for resistance electrically welded plates is vast, encompassing numerous industrial sectors, including automotive, aerospace, electronics, household appliances, and many others [7-8-9]. In the automotive industry, for example, resistance electrically welded plates are widely used to assemble body and chassis components, ensuring a robust and lightweight structure [1]. Similarly, in the aerospace sector, this welding method is employed to join lightweight components while preserving their structural integrity. This method also offers economic advantages in terms of production costs

*** Corresponding author:** Cherfi Mohamed, ***E-mail address:*** *mohamed.cherfi@univ-sba.dz*

and maintenance [10-11]. However, the optimal performance of this technique heavily relies on the nature of the materials used. This is where Dual Phase (DP) steels come into play as a strategic material choice [12-13]. Dual Phase steels are specially designed metallic alloys that provide an optimal balance between strength and ductility [14-15]. In this study, the focus is on DP 450 and DP 980, as these two types of materials used in the spot-welding industry play a significant role in the fabrication of robust and efficient metal structures [16-17]. DP 450 and DP 980 steels have emerged as preferred choices due to their exceptional mechanical properties and adaptability to the specific requirements of spot welding [18].

The cross-tension test and the tensile-shear test are commonly employed in the automotive industry to characterize the quasi-static behavior of a welded spot. These tests enable the measurement of the force required to fracture the welded spot under the specific loading condition, as well as to determine its failure mode. The force at fracture is commonly referred to as CTS (Cross Tension Strength) in the case of the cross-tension test, and as TSS (Tensile Shear Strength) for the tensile-shear test [20]. Shear tensile tests hold a fundamental place in the field of spot welding, where the assembly of metal plates is a common practice. This specific testing method aims to assess the strength and durability of welded joints by subjecting them to loads applied in a direction perpendicular to the axis of the weld [19]. This approach provides crucial insights into the ability of welds to withstand shear stresses, a type of loading often encountered in real industrial applications. In this study, shear tensile testing simulates the stresses to which welds are subjected when a force is applied perpendicular to the weld axis. This test determines the ability of a welded joint to resist shear stresses, which is essential for evaluating its strength under real-world conditions [20].

Furthermore, numerical simulations of this test offer the advantage of virtually replicating this process, enabling the analysis of stresses and deformations at the microscopic scale. Notably, the finite element analysis software ABAQUS has proven to be a valuable tool for the in-depth analysis of the mechanical properties of welded plates [21-22]. This approach allows for the virtual modeling of complex interactions between materials and stresses, providing a detailed insight into the behavior of welds under various conditions [23-24]. During these simulations, two stress measures play a crucial role in the analysis: Von Mises stresses and maximum principal stresses. Von Mises stresses provide an assessment of the plastic deformation of a material, while maximum principal stresses reveal the directions and magnitudes of the most significant loads [25]. The study of these parameters helps predict the potential failure point and identify stress concentration areas, which can guide design modifications to optimize weld performance. Furthermore, the use of the J-integral contour in numerical simulations of welded plates is of great importance [18]. This parameter (J-integral) serves as an indicator of fracture resistance in the presence of cracks or defects. Analyzing the J-integral contour helps detect stress concentration areas around potential cracks, thus aiding in anticipating potential failures and reinforcing designs.

This study introduces a novel approach to analyze the stress distribution and deformation characteristics in and around the weld zone of resistance spot-welded (RSW) dual-phase steels (DP450 and DP980) using advanced computational techniques. Specifically, we leverage the powerful capabilities of ABAQUS to perform detailed evaluations of the J-integral within the weld region, which provides a quantitative measure of the intensity of the elastoplastic stress field near potential crack sites. This innovative use of the J-integral, combined with the application of the von Mises criterion and the maximum principal stress criterion, enables us to pinpoint critical stress concentration areas and assess the likelihood of crack initiation and propagation with unprecedented precision.

Furthermore, our study goes beyond traditional stress analysis by evaluating the overall reliability of the weld joint. This allows us to develop a more robust understanding of the factors influencing weld joint failure and to propose specific safety factors that are necessary to ensure adequate reliability under various service conditions.

2. Method

2.1. Geometric model

The geometric model is a set of physical and mechanical or thermal data used based on previous studies in the field on which we want to generate the latter. The digital model for this study focuses on the

creation of two plates welded by point. This model is inspired by the experimental study of Sylvain DANCETTE and Habib LEBBAL, who use dual-phase steel types to model the behavior of welded plates. This model is based on the combination of three essential parts of each weld point (the base metal BM, the melted metal MM, and the heat-affected zone HAZ) [26] [27]. Our objective is focused on comparing 02 spot-welded plates. These two plates have the same dimensions as shown in the figure 1 (125 mm in length and 38 mm in width for each piece with a 38 mm overlap and a molten core diameter of around 2.5 mm).

To provide a detailed description of the geometric model used in this study, we will describe the following elements:

2.1.1. Base Metal (BM)

– The base metal represents the primary part of the plate that is not directly affected by the welding process.

– In this model, it is dual-phase steel, selected for its favorable mechanical properties and performance under spot welding conditions.

2.1.2. Melted Metal (MM)

– The melted metal is the region that undergoes complete fusion during the welding process.

– This area is crucial as it determines the strength and quality of the weld. For this model, the diameter of the molten zone is approximately 2.5 mm.

2.1.3. Heat-Affected Zone (HAZ)

– The heat-affected zone is the region surrounding the melted metal which, although not melted, has undergone microstructural changes and alterations in mechanical properties due to heat exposure.

Each plate measures 125 mm in length and 38 mm in width, with an overlap area of 38 mm where spot welding is performed. These dimensions are chosen to match experimental conditions and reference studies, ensuring the validity of comparisons and results [26] [27]. The geometric model thus defined allows for precise simulation of the behavior of welded plates under different load conditions and helps to understand potential failure mechanisms. The results of this modeling will provide valuable insights for optimizing welding processes and improving the performance of welded structures. The Figure 1 presents a schematic illustration of the geometric model used, showing the dimensions of the plates and the spot-welding areas. This visual representation helps to understand the exact configuration of the elements in the study.

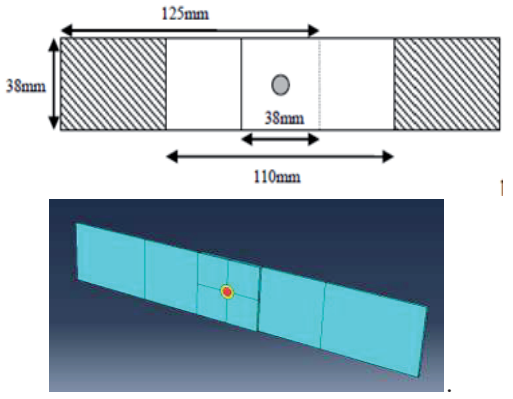

Figure 1: geometrical model.

2.2. Mechanical properties

The results presented in Figure 2 allowed us to deduce the mechanical properties of each material and for each phase state (base metal, molten metal and heat-affected zone (HAZ)). In this study, the mechanical properties were introduced based on the experimental work of Dr. Sylvain Dancette [26]. According to Dr. Dancette's results, tensile tests were conducted on DP450 and DP980 plates according to their thermal cycles to determine the mechanical behavior law for each material in the three phases. The stress-strain curves obtained (Figure 2) show that tensile strength and elongation vary significantly depending on the thermal treatment. For DP450, the maximum strength is reached after thermal treatment at 1200 °C with rapid cooling, while for DP980, high strength is also observed at 1200 °C with water cooling. These data were essential for calibrating the FEM model and ensuring that the simulations accurately reflect the real behavior of the materials under various loading conditions. The specific mechanical properties introduced into the model include Young's modulus, Poisson's ratio, yield strength, and ultimate tensile strength, adjusted for each phase state according to the applied thermal cycles.

The methodology for preparing the joint samples and the welding parameters were rigorously defined to ensure reproducibility and precision in our study. The samples were prepared from DP450 and DP980 dual-phase steel sheets, each 1.5 mm thick, cut to standard dimensions of 125 mm x 38 mm with a 38 mm overlap. Before welding, the sheet surfaces were cleaned with acetone to remove any contaminants. Resistance spot welding was performed using a medium-frequency DC welder, with a welding current of

6 kA, a weld time of 20 cycles, and an electrode force of 3 kN. Copper electrodes were applied to the sheet surfaces to generate the necessary heat for material fusion, followed by maintaining pressure for a few cycles to allow solidification. For some samples, post-weld heat treatment was applied (heating at 200 °C for 1 hour followed by air cooling) to study the effects of thermal cycles on joint properties. Each welded joint was inspected visually and with ultrasonic testing to detect defects, and tensile-shear tests were conducted to evaluate the mechanical properties, with force-displacement curves recorded and analyzed.

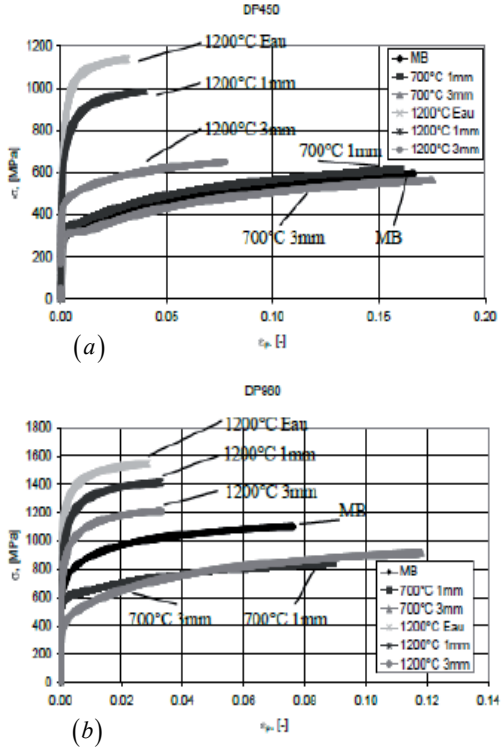

Figure 2: Properties and materials [26]

These data were essential for calibrating the FEM model and ensuring that the simulations accurately reflect the real behavior of the materials under various loading conditions. The specific mechanical properties introduced into the model include Young's modulus, Poisson's ratio, yield strength, and ultimate tensile strength, as detailed in Table 1.

Table 1: Properties of materials DP450 (a) and DP950 (b)[26]

Properties	*BASE METAL*	*MOLTEN METAL*	*HEAT AFFECTED ZONE METAL*
Young'smodulus (GPa)	70	465	114
Poisson's ratio	0.3	0.3	0.3
Yield stress (MPa)	303	683	336
MAX stress (MPa)	601	981	618

(a)

Properties	*BASE METAL*	*MOLTEN METAL*	*HEAT AFFECTED ZONE METAL*
Young'smodulus (GPa)	416	444	250
Poisson's ratio	0.3	0.3	0.3
Yield stress (MPa)	719	888	430
MAX stress (MPa)	1103	1209	908

(b)

2.3. Boundary conditions and meshing model

The boundary conditions imposed in this study are illustrated in the figure 3 (a):

- *In terms of fixation: embbeding an imposed fixture and a load imposed in MPa on the opposite side.*
- *In terms of displacement: Zero displacement in both the Y and Z axes, while displacement is allowed along the X-axis.*

The figure3 (b) illustrates the meshing of the different components of the welded plate. Following the principle of convergence and the precision of the results in this study for generating the geometric model, we proceeded with mesh refinement in the various constituents of the plate.

In this context, the ABAQUS computational code afforded us the ability to perform mesh refinement comprehensively across various regions and orientations. In this study, we implemented a C3D8R element, leading to a total of 23082 such elements within the complete model.

The FEM numerical model developed in this study accurately simulates the mechanical behavior of resistance spot-welded joints in DP450 and DP980 steels(Figure 3). The contact between the molten metal and the adjacent joint zones was defined using the 'contact tie' method in ABAQUS, ensuring a perfect bond between the contact surfaces and precise load transfer. The other interfaces are assumed to be free to allow realistic interaction under stress. 3D solid elements (C3D8R) with reduced integration were used to capture the stress distribution and deformations, with mesh

refinement in high-stress gradient areas.

The accuracy of the calculations in this study has been rigorously validated through a combination of experimental data and numerical simulations. The finite element modeling (FEM) was calibrated using mechanical properties derived from experimental stress-strain curves for DP450 and DP980 steels, as shown in Figure 2 and Table 1. The primary sources of data for calibration included Young's modulus, Poisson's ratio, yield strength, and ultimate tensile strength.

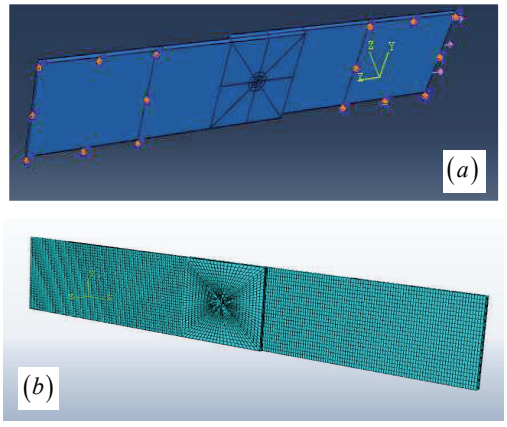

Figure 3: (a) boundary conditions and,(b)mesh model

3. Results and Discussion

3.1. Study of the stress state

3.1. 1. Von Mises stress

The simulation of the tensile shear test for these two types of materials, DP450 and DP980, allowed us to study and understand the mechanical behavior of these materials during spot welding. The ABAQUS computational code provides us with the ability to visualize highly stressed areas and categorize them using a color code, which degrades from blue to green and finally to red. This color code helps determine areas that are highly and less stressed.

The figure 4 (a) and (b) represent the variation of equivalent stress (VON MISES), maximum principal stress, and normal stresses on the facets (S11, S22, S33) as a function of applied load from 20 to 180 MPa. We observe that the maximum values for both welded plates are recorded by the maximum principal stress and S11, following the same trend. These stresses are almost comparable for both materials, at approximately 864 and 1000 MPa. These values continue to increase with the applied load. Meanwhile, the equivalent stress remains lower

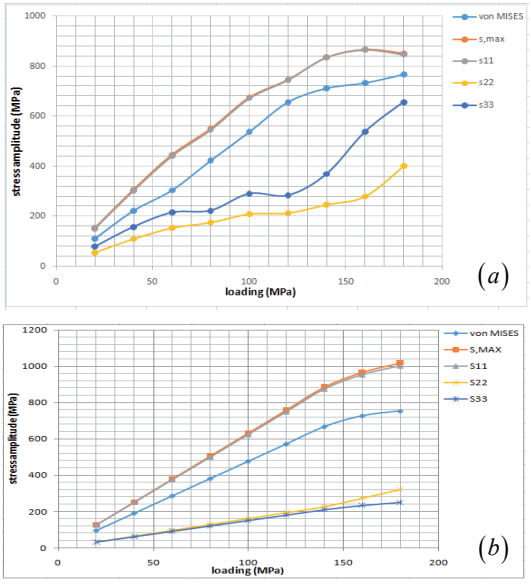

Figure 4: Distribution of stress as a function of load: (a) (DP450), (b) (DP980)

and also increases with the applied load, reaching a maximum value at an amplitude of 180 MPa for both DP450 and DP980. The normal stresses S22 and S33 are less significant compared to the first set of stresses. This increase in stress intensity is primarily due to the applied load and boundary conditions imposed, and secondarily to the mechanical properties of the three welding zones.

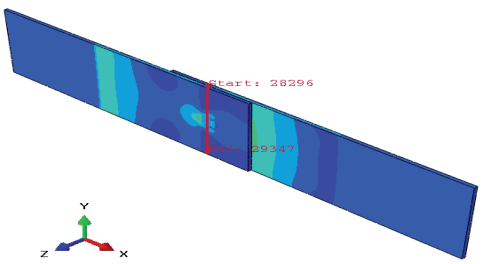

Figure 5: Load effect (transverse plot)

The figure 5 below represents the schematization of the transverse direction in our study. It is the axis that passes through the midline between the two sheets at the overlap level, crossing the heat-affected zone and the weld point (melted metal). This axis was created with the purpose of visualizing the evolution of equivalent stress at the contact points between the two plates.

The figure 6 represent the variation of equivalent stress for the two materials DP450 and DP980 as a function of overlap (38 mm) for four loading modes,

ranging from 20 MPa to 180 MPa. In this simulation section, we modeled stress distribution in the radial and transversal directions to visualize the distribution of equivalent stress. We observed that the stress distribution is symmetrical with respect to the fusion point for both types of materials. The stress intensity gradually increases as it approaches the fusion point and the Heat-Affected Zone (HAZ), and it decreases as it moves away from it. These values are nearly comparable, with 652 MPa for DP450 and 600 MPa for DP980. The areas that remain sensitive to variations in stress intensity are located at the contact interfaces MB-HAZ and HAZ-MM. However, for DP980, a significant stress concentration is noticeable at the BM-HAZ interface compared to DP450, which records a maximum value at the HAZ-MM interface.

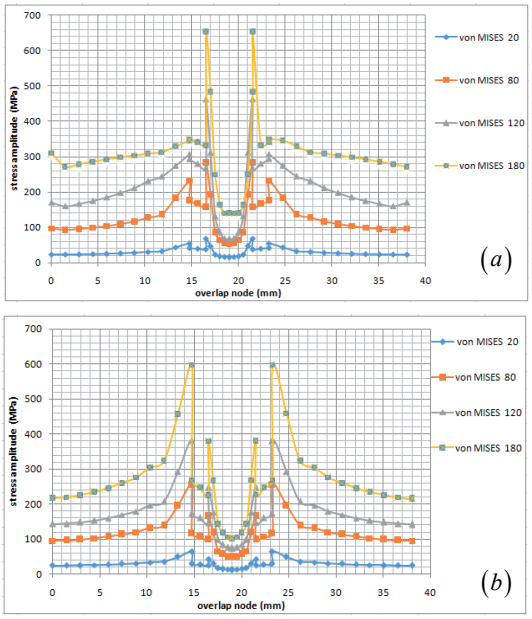

Figure 6: Evolution of Von Mises stress as a function of transverse overlap nodes for: (a) DP450, (b) DP980

3.1. 2. Distribution for the overall model

It is essential to understand the effect of the load on the variation of the principal stress to assess the risks of degradation of the weld joint and the welded plates. To do this, we have represented the stress distribution in the form of a histogram that shows the distribution of the maximum principal stress as a function of the applied load. In blue, we represent the stresses associated with the load that does not exceed the limit, unlike the red bars in the histogram, which indicate exceeding the limit. This variation has been compared to the yield strength of each material (BM, HAZ, MM) to determine the areas with high stress intensity that are susceptible to damage. The goal of this analysis is to identify areas where microcracks could appear due to high stresses. These microcracks can then lead to degradation of the weld joint, which has a negative impact on the welded plates. By examining the results of this analysis, it will be possible to locate critical areas and take preventive measures to avoid potential damage (see figure 7 (a), and (b)).

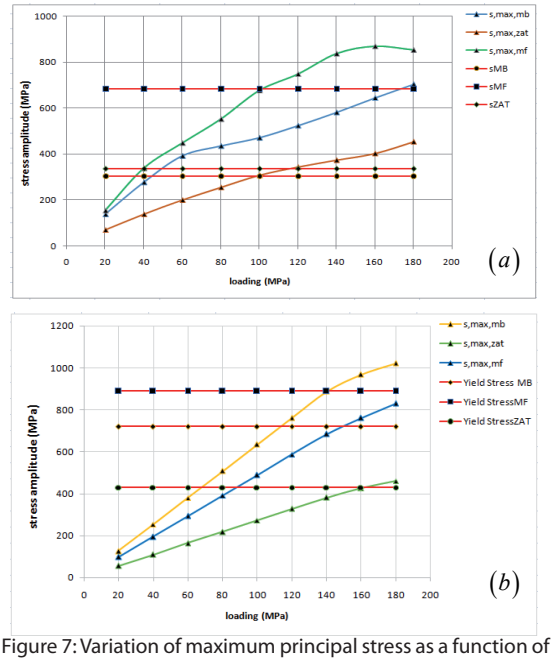

Figure 7: Variation of maximum principal stress as a function of applied load (a) (DP 450), (b) (DP980)

3.1. 3. Histogram of max principal stress

Both histograms depict the relationship between stress and applied load inMPa for the DP450 and DP980 materials. When analyzing the characteristics of the plates (BM), it is observed that DP980 has a higher yield strength than DP450, reaching approximately 300 and 700MPa, respectively. For the first material, the limit is exceeded beyond 60MPa, while the second material records an amplitude of 120MPa before crossing the yield limit. Beyond these load values, the plates begin to deform until they eventually fracture (see figure 8 (a), (b)).

Examining the heat-affected zone (HAZ), it is found that DP450 extends up to 120MPa before losing its elasticity, while DP980 retains its elasticity up to 180MPa (see figure 9 (a), (b)). In contrast, the melted metal (MM) shows signs of damage beyond

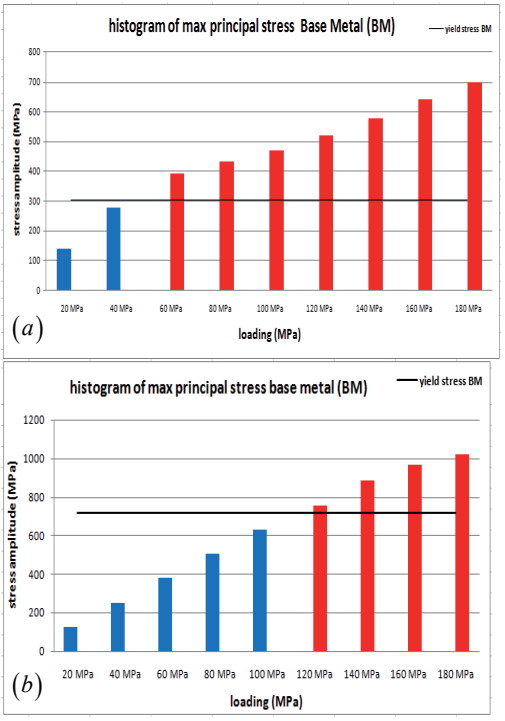

Figure 8: Histogram of max principal stress in the base metal:(a) (DP450) and (b) (DP 980)

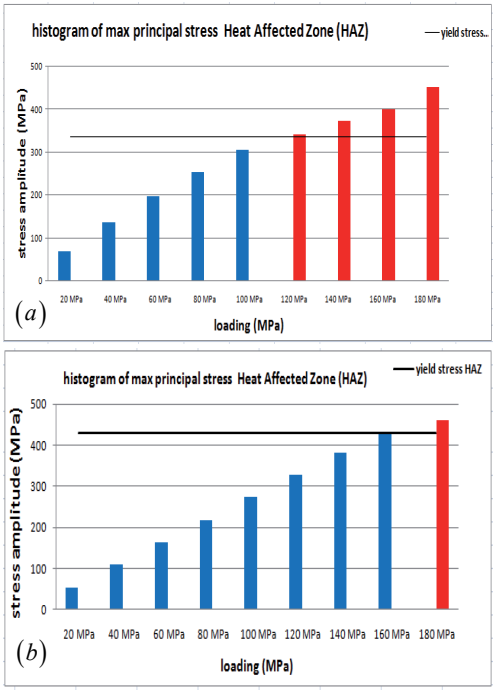

Figure 9: Histogram of max principal stress in heat affected zone:(a) (DP450) and (b) (DP 980)

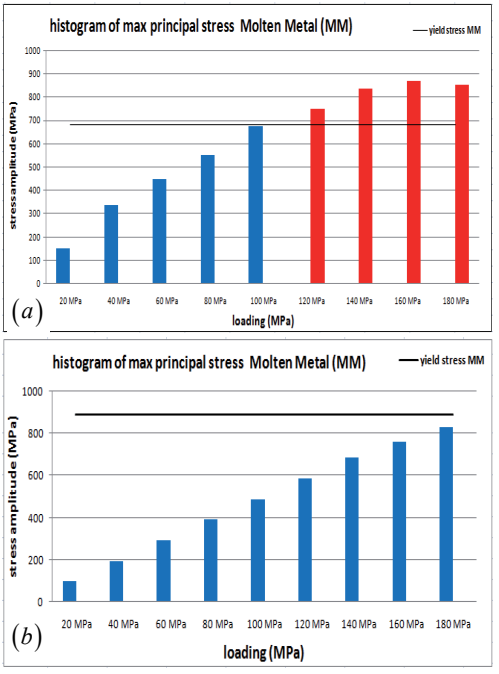

Figure 10: Histogram of max principal stress in molten metal: (a) (DP450) and (b) (DP 980)

120MPa for the first material, while the melted zone of DP980, where the weld point is located, remains intact. Across the entire spot-welded joint, the damaged area primarily concentrates in the base metal due to its lower limit compared to that of ZAT and MF (see figure 10 (a), (b)).. Therefore, it is likely that microcracks may appear in the base metal. This information is crucial to consider when evaluating the strength and durability of the spot-welded joint.

3.2. Fracture behavior of welded plates

The study of the fracture behavior of resistance-welded components, especially alloys DP450 and DP980, is essential to ensure the reliability and durability of welded structures in demanding industrial applications. When components are subjected to mechanical loads, the resulting stresses can exceed tolerated limits, leading to the occurrence of damage and, ultimately, fracture [28]. In-depth analysis of stress-strain curves and histograms of principal stresses is crucial for understanding fracture mechanisms and improving the design and fabrication of welded components. A comprehensive study of the fracture behavior of DP450 and DP980 resistance-welded components using stress-strain curve data and histograms of principal stresses will provide a better understanding

of the fracture mechanisms associated with these alloys. This will provide valuable insights for optimizing welding parameters, material selection, and component design to minimize the risk of premature fracture (see figure 11).

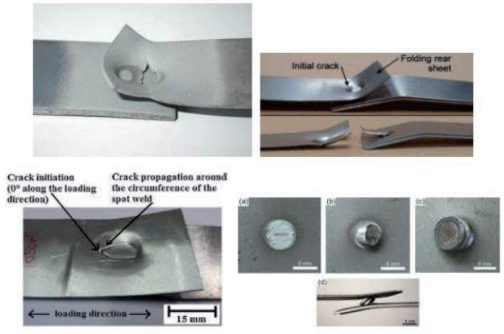

Figure 11: Fracture behavior of welded plates (shear tensile test) [29][30]

Stress-strain curves and histograms of principal stresses are valuable tools for assessing the stresses applied to welded components. These data allow us to visualize the stress distribution and identify areas where stresses can reach critical levels. When stresses exceed the tolerated limit, damage zones can form, such as microcracks or excessive plastic deformations, which can lead to a degradation of the component's strength and, ultimately, fracture. During this process, it is essential to monitor the appearance of cracks in the welds to prevent premature failures.

In this study, we will focus on the consequences of the crack detected in the base metal, as it is presented as the first material susceptible to damage in the BM-HAZ-MM chain. This crack, of a yet-to-be-determined size (10mm), will be subjected to continuous loading to study the evolution of the J-parameter. The goal of this study is to track the crack's progression and assess its impact on the material's performance. By monitoring the J-parameter during continuous loading, we will be able to quantify the crack's growth and obtain crucial information about its propagation. This will also allow us to take preventive measures and design tailored solutions to enhance the base metal's strength. This study is a significant step in as it will help us better understand base material failures (see figure 11).

The use of the J-integral as a parameter to evaluate crack opening is a commonly used approach in weld joint analysis. The J-integral is a

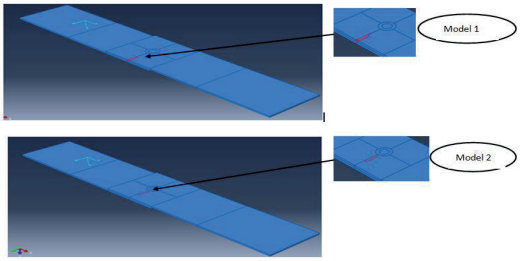

Figure 12: Model 1 and model 2 of fracture modeling

parameter used to quantify crack propagation in welds, representing the total energy released per unit area as a crack propagates in a material. By measuring the J-integral, it is possible to assess crack opening and predict crack propagation behavior in the weld joint. Understanding the relationship between the J-integral and crack opening would enable the determination of optimal welding parameters that minimize the risk of cracking and improve weld quality. Furthermore, this approach would allow for the assessment of weld joint durability and identification of critical areas requiring special attention during the design and fabrication of welded components.

In this study, we have developed two distinct models while maintaining the dimensions of our base model, except for the point of crack initiation. The first model aims to simulate the fracture mode starting from the free edge of the plate, while the second model initiates the crack from the interface of the heat-affected zone. The objective of this approach is to compare fracture behaviors in these two different scenarios (see figure 12).

By modeling the crack initiation from the free edge of the plate, we seek to evaluate the material's strength under loading conditions that simulate a realistic situation. On the other hand, by initiating the crack from the interface of the heat-affected zone, we focus on the impact of thermal conditions on crack propagation. This approach allows us to understand how the characteristics of the heat-affected zone influence the material's strength.

By using these two models, we will be able to compare the obtained results and draw meaningful conclusions about fracture mechanisms and the factors influencing crack propagation. This information will be crucial for making informed decisions regarding material design and durability improvement.

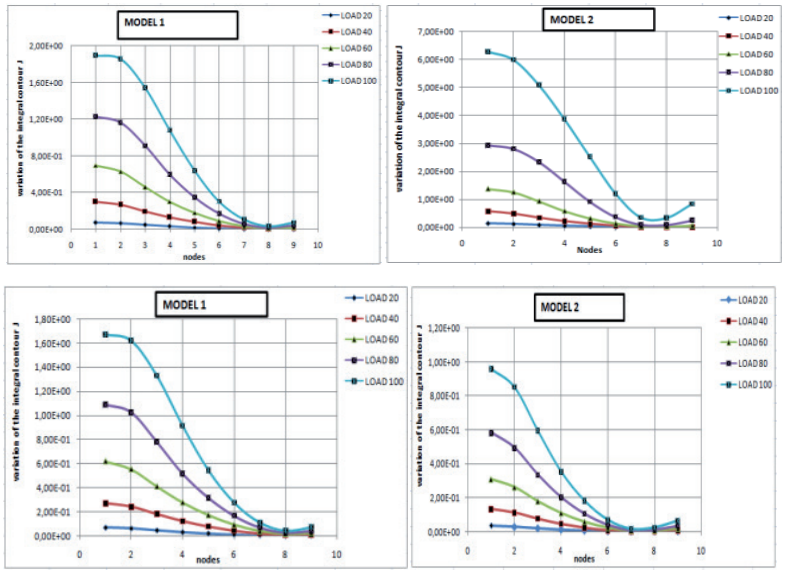

Figure 13: Evolution of the J-parameter (Model 1 and 2) (a) (DP450) and (b) (980)

Model 1:

– *The J-integral contour results for Model 1 are comparable for both materials, DP450 and DP980.*

– *The maximum J-integral result for Model 1 with DP450 is 1.89 (kJ/m²) for a load of 100 MPa.*

– *The maximum J-integral result for Model 1 with DP980 is 1.6 (kJ/m²) for a load of 100 MPa.*

– *Model 1 poses no risk to the assembly of the two spot-welded plates, whether for the DP450 or DP980 material. This means that the crack is not fully open, and the rupture of the base metal outside the weld point is not favored.*

Model 2:

– *The maximum J-integral result for Model 2 with DP450 is 6.28 (kJ/m²) for a load of 100 MPa.*

– *The maximum J-integral result for Model 2 with DP980 is 0.96 (kJ/m²) for a load of 100 MPa.*

– *For DP450 material in Model 2, the high J-integral values indicate that the crack is fully open. This favors the rupture of the base metal outside the weld point and can lead to the failure of the assembly of the two spot-welded plates.*

– *For DP980 material in Model 2, the J-integral values remain less significant, comparable to 1 (kJ/m²) for a load of 100 MPa. This suggests that the crack is not fully open, and the risk of rupture of the base metal outside the weld point is lower compared to DP450 in Model 2.*

4. Conclusions

In order to assess the mechanical strength of spot welds in steel used in the automotive industry, we undertook one of the most comprehensive tests, namely the shear tensile test, with the aim of determining how electric resistance welded plates behave when they reach the point of rupture. For this purpose, we developed a detailed numerical model using the ABAQUS calculation software, which faithfully reproduces the geometric model applied during the tensile test. It is important to emphasize that this study focused on analyzing the behavior of DP450 and DP980 steels in the elastoplastic domain, which provides valuable information about their strength and performance when subjected to mechanical stresses.

The results presented in this article include both finite element modeling (FEM) and experimental tests, focusing on the failure modes of resistance spot-welded dual-phase steels (DP450 and DP980). The experimental tests were primarily used as a data source to calibrate our FEM model. Mechanical properties, such as Young's modulus, Poisson's ratio, yield strength, and maximum stress, were derived from the stress-strain curves obtained experimentally (Figure 2 and Table 1). The FEM simulations then predicted the failure modes observed experimentally, such as interfacial fractures for DP450 and nugget pullout failures for DP980. Comparative analysis revealed that DP980 exhibited better joint strength and greater resistance to crack propagation compared to DP450. By using experimental data for calibration and relying on numerical simulations, our study demonstrates the

reliability of FEM as a predictive tool to optimize welding techniques and improve joint performance.

Through this approach combining experimental testing and numerical modeling, we are able to more accurately estimate the strength of steel spot welds, contributing to the continuous improvement of the safety and durability of automotive vehicles.

The results obtained allow us to conclude that:

– *The tensile test induces a significant increase in stress in the region of the plate near the interfaces of Base Metal-ZAT and ZAT-Melted Metal.*

– *The Von Mises stress records a comparable range for both materials, ranging from 900 to 1000 MPa.*

– *Maximum principal stress and normal stress along facet 1 exhibit similar trends for the shear tensile test and record higher values than other types such as S22 and S33.*

– *The transverse plot yields considerably higher values at the MB-ZAT and ZAT-MF interfaces, which is due to differences in stiffness among the three zones.*

– *In spot welding, the base metal represents the weakest link compared to MF and ZAT, as stress intensity primarily localizes at the MB-ZAT interface for a low applied load.*

– *Stress intensity localizes at the MB-ZAT interface, leading to the initiation of damage through the clustering of microcracks in the base metal.*

– *In both fracture models, the behavior is identical, except for Model 2 for DP450, which exhibits a notable behavior with a high J-parameter.*

– *The weld point remains intact for both models, except in cases where the crack is located close to the weld point in the direction of the load; in this case, the joint is susceptible to deterioration regardless of the material used.*

The conclusions of this study are most directly applicable to the DP450 and DP980 grades of sheet metal under the specific welding parameters used in the experiments. Although the FEM model and the experimental data provide a robust basis for understanding the behavior of these materials, further studies would be needed to validate the findings under different welding conditions or with other grades of sheet metal. This research lays the groundwork for optimizing welding techniques for DP450 and DP980, but additional investigations are necessary to extend these conclusions to a broader range of materials and parameters.

Acknowledgments

Firstly we acknowledge the Ministry of Higher Education and Scientific Research, Algeria, for technical and financial support; secondly we would like to express our sincere gratitude to the editorial team and reviewers of Acta Mechanica Slovaca for their valuable feedback and guidance throughout the publication process. Their expertise and constructive comments greatly contributed to the improvement of this manuscript. We also acknowledge the support received from faculty of technology of SIDI BEL ABBES and laboratory of mechanics and physics of materials for their financial assistance, which made this research possible.

References

[1] FeujofackKemda, B. V. (2020). Modélisation, optimisation et surveillance en temps réel du procédé de soudage par résistance par points appliqué aux plaques minces pour l'industrie automobile (Doctoral dissertation, Université du Québec à Rimouski).

[2] Dickinson, D. W., Franklin, J. E., &Stanya, A. (1980). Characterization of spot welding behavior by dynamic electrical parameter monitoring. Welding Journal, 59(6), 170.

[3] Aslanlar, S., Ogur, A., Ozsarac, U., &Ilhan, E. (2008). Welding time effect on mechanical properties of automotive sheets in electrical resistance spot welding. Materials & Design, 29(7), 1427-1431.

[4] Luo, Y., Liu, J., Xu, H., Xiong, C., & Liu, L. (2009). Regression modeling and process analysis of resistance spot welding on galvanized steel sheet. Materials & Design, 30(7), 2547-2555.

[5] Hamidinejad, S. M., Kolahan, F., &Kokabi, A. H. (2012). The modeling and process analysis of resistance spot welding on galvanized steel sheets used in car body manufacturing. Materials & Design, 34, 759-767.

[6] Khan, J. A., Xu, L., Chao, Y. J., & Broach, K. (2000). Numerical simulation of resistance spot welding process. Numerical Heat Transfer: Part A: Applications, 37(5), 425-446.

[7] M. S. Khan,S. D. Bhole, D. L. Chen,E. Biro,G. Boudreau&J. van Deventer. (2013).Welding behaviour, microstructure and mechanical properties of dissimilar resistance spot welds between galvannealed HSLA350 and DP600 steels.Science and Technology of Welding and Joining , volume 14, NO 7 616

[8] Wang, J., Wang, H. P., Lu, F., Carlson, B. E., & Sigler, D. R. (2015). Analysis of Al-steel resistance spot welding process by developing a fully coupled multi-physics simulation model. International Journal of Heat and Mass Transfer, 89, 1061-1072.

[9] Baltazar Hernandez, V. H., Panda, S. K., Okita, Y., & Zhou, N. Y. (2010). A study on heat affected zone softening in resistance spot welded dual phase steel by nanoindentation. Journal of Materials Science, 45, 1638-1647.

[10] Bagheri, B., Abbasi, M., Abdollahzadeh, A., &Moghaddam, A. O. (2021). Numerical modeling and experimental analysis

of water jet spot welding and friction stir spot welding: a comparative study. Journal of Materials Engineering and Performance, 30, 1454-1471.

[11] Brizes, E., Jaskowiak, J., Abke, T., Ghassemi-Armaki, H., & Ramirez, A. J. (2021). Evaluation of heat transfer within numerical models of resistance spot welding using high-speed thermography. Journal of Materials Processing Technology, 297, 117276.

[12] Sam, S., &Shome, M. (2010). Static and fatigue performance of weld bonded dual phase steel sheets. Science and Technology of Welding and Joining, 15(3), 242-247.

[13] Eshraghi, M., Tschopp, M. A., Zaeem, M. A., &Felicelli, S. D. (2014). Effect of resistance spot welding parameters on weld pool properties in a DP600 dual-phase steel: A parametric study using thermomechanically-coupled finite element analysis. Materials & Design (1980-2015), 56, 387-397.

[14] Wan, X., Wang, Y., & Zhang, P. (2017). Numerical simulation on deformation and stress variation in resistance spot welding of dual-phase steel. The International Journal of Advanced Manufacturing Technology, 92, 2619-2629.

[15] Ren, S., Huang, W., Ma, N., Watanabe, G., Zhang, Z., & Deng, W. (2023). Numerical modeling from process to residual stress induced in resistance spot welding of DP980 steel. The International Journal of Advanced Manufacturing Technology, 125(7), 3563-3576.

[16] Song, J., Zhu, L., Wang, J., Lu, Y., Ma, C., Han, J., & Jiang, Z. (2023). Physical simulation and numerical simulation of flash butt welding for innovative dual phase steel DP590: a comparative study. Materials, 16(9), 3513.

[17] Demir, B., Ali, K. B., Gürün, H., &Acarer, M. (2023). An investigation of the shearing performance and sheared surface characterisation of ultra-strength DP steel-Al explosive welded plate composite. The International Journal of Advanced Manufacturing Technology, 126(5), 1845-1861.

[18] M., Goktas, M., Acarer, M., &Demir, B. (2023). Finite element modelling of the fatigue damage in an explosive welded Al-dual-phase steel. Materials Testing, 65(5), 787-801.

[19] Rajalingam, P., Rajakumar, S., Balasubramanian, V., Sonar, T., &Kavitha, S. (2023). Tensile shear fracture load bearing capability, softening of HAZ and microstructural characteristics of resistance spot welded DP-1000 steel joints. Materials Testing, 65(1), 94-110

[20] Gandhi, A. D., Kundu, A., Kumar, R., &Chakraborti, P. C. (2023). Effect of Heat Input on the Weld Thermal Cycle, Microstructure, Tensile Damage and Fracture Behavior of Pulsed Laser-Welded Dual-Phase Steel. Journal of Materials Engineering and Performance, 1-18.

[21] Rao, Z., Liu, L., Wang, Y., Ou, L., & Liu, J. (2021). Preventing nugget shifting in joining of dissimilar steels via resistance element welding: a numerical simulation. The International Journal of Advanced Manufacturing Technology, 117, 227-241.

[22] Reddy Gillela, P. K., Jaidi, J., Gude, V., Pathak, S. K., & Srivastava, D. (2023). A numerical study on contact conditions, dynamic resistance, and nugget size of resistance spot weld joints of AISI 1008 steel sheets. Numerical Heat Transfer, Part A: Applications, 84(2), 122-140.

[23] Zhou, K., Yu, W., Wang, G., &Ivanov, M. (2023). Comparative analysis between multi-pulse and constant welding current for resistance spot welding process. Journal of Materials Science, 58(6), 2853-2875.

[24] Tan, N., Hong, J., Lei, M., Jin, X., Zheng, H., &Luo, Z. (2020). Tensile-shear fracture behaviour of resistance spot-welded hot stamping sheet steel with Al–Si coating. Science and Technology of Welding and Joining, 25(6), 525-534.

[25] Palmonella, M., Friswell, M. I., Mottershead, J. E., & Lees, A. W. (2005). Finite element models of spot welds in structural dynamics: review and updating. Computers & structures, 83(8-9), 648-661.

[26] Dancette, S. (2009). Comportement mécanique des soudures par points: mécanismes et stratégies de prédiction dans le cas des tôles en acier pour automobile. Lyon: École doctorale matériaux de Lyon.

[27] LEBBAL, H. (2016). Analyse expérimentale et modélisation du comportement thermodynamique des aciers inoxydables et dual phase. Application au procédé du soudage par résistance par point (Doctoral dissertation).

[28] Kumar, P., Pathak, H., & Singh, A. (2021). Fatigue crack growth behavior of thermo-mechanically processed AA 5754: experiment and extended finite element method simulation. Mechanics of Advanced Materials and Structures, 28(1), 88-101.

[29] Nielsen, C. V., Friis, K. S., Zhang, W., & Bay, N. (2011). Three-sheet spot welding of advanced high-strength steels. Welding journal, 90(2), 32s-40s.

[30] Brožek, M., Nováková, A., &Niedermeier, O. (2017). Resistance Spot Welding of Steel Sheets of the Same and Different Thickness, 65(3).